Photochemical Upconversion in Water Using Cu(I) MLCT Excited States: Role of Energy Shuttling at the Micellar/Water Interface

R. Fayad, Anh Thy Bui, S.G. Shepard, F.N. Castellano

Photochemical Upconversion in Water using Cu(I) MLCT Excited States: Role of Energy Shuttling at the Micellar/Water Interface

Remi Fayad,[a] Anh Thy Bui,[b] Samuel G. Shepard,[a] Felix N. Castellano [a]*

[a]Department of Chemistry, North Carolina State University, Raleigh, North Carolina 27695-8204, United States.

[b]Current Address: Institut des Sciences Chimiques, Université de Rennes 1, Rennes, France

Keywords: *Photochemical upconversion, triplet-triplet annihilation, copper(I) MLCT excited states, earth-abundant photosensitizer, energy transfer*

Supporting Information Placeholder

ABSTRACT: Photochemical upconversion (UC) through triplet-triplet annihilation (TTA), which employs a visible absorbing triplet photosensitizer and an annihilator, is a process that generates a high energy photon from two lower energy photons. TTA-UC has been largely developed in pure organic solvents and solid-state polymeric constructs while featuring near exclusive use of rare and expensive metals within the photosensitizer. In this current investigation, we demonstrate that TTA-UC from the long lifetime earth-abundant photosensitizer $[Cu(dsbtmp)_2](PF)_6$ (dsbtmp = 2,9-di(*sec*-butyl)-3,4,7,8-tetramethyl-1,10-phenanthroline), abbreviated as Cu-PS, functions in water through encapsulation within a cationic-based assembly. Cetyltrimethylammonium bromide (CTAB) was the surfactant of choice as it electrostatically binds the negatively charged water-soluble 10-phenylanthracene-9-carboxylate (PAC) acceptor/annihilator and ultimately facilitated energy transfer across the interface. Efficient and diffusion limited triplet-triplet energy transfer (TTET) from Cu-PS to the PAC acceptor was achieved in this aqueous assembly. Unfortunately, the hindered mobility of the PAC moieties ultimately hampered the annihilation process and this was reflected in attenuated TTA rates and efficiencies. The combined experimental data illustrated that the water-soluble PAC acceptor was able to vectorially deliver the excited state energy stored in Cu-PS across the interface into the bulk aqueous solution by engaging in excited state electron transfer with methyl viologen acceptors. These results are important for remotely operating photoredox reactions in water while rendering a photosensitizer spatially isolated in the hydrophobic core of a micelle.

Introduction

Extensive research has been conducted on photochemical upconversion based on triplet-triplet annihilation (TTA-UC), a multistep process that combines the energies of two low-energy photons to produce one high-energy photon. TTA-UC has met the needs of a multitude of applications from enhancing the photoresponse to sub-band gap light in a variety of solar energy devices,[1-4] to bioimaging and photodynamic therapy.[5-9] TTA-UC was first reported by Parker and Hatchard in the early 1960s and was based solely on organic sensitizers and annihilators.[10] These systems suffered from low efficiency due to low triplet yields in the photosensitizer. The interest in photochemical upconversion was revived by the inclusion of inorganic transition metal complexes in TTA-UC systems. Due to their high molar absorptivity and efficient ISC rates, transition metal complexes are now the most widely used photosensitizers for TTA, particularly those based on Ru-, Pd-, Pt- complexes.[11-12] In 2013, we successfully integrated Cu(I) MLCT excited states into upconversion schemes providing an earth-abundant alternative to the more precious 2nd and 3rd row transition metals, namely using $Cu(dpp)_2^+$ (dpp = 2,9-diphenyl-1,10-phenanthroline)[13] and shortly after with $Cu(dsbtmp)_2^+$, (dsbtmp = 2,9-di(*sec*-butyl)-3,4,7,8-tetramethyl-1,10-phenanthroline).[14]

Recently, the photocatalytic applications of TTA-UC have been increasingly investigated.[15-16] In synthetic applications, particularly on an industrial scale, water is a desirable "green" solvent, because it eliminates the considerable waste in the form of unrecoverable organic solvents. However, although there are many reports on upconversion both in solution and in solid matrices in the literature, very few of them operate with molecular photosensitizers and annihilators in aqueous solution. The difficulty in realizing TTA-UC in water stems from two main challenges. First, both the photosensitizer and annihilator molecules are generally insoluble in water due to their non-polar character. Second, a highly polar solvent favors electron transfer reactions, which emerge as a competing process against the desired TTET reaction between the photosensitizer and the annihilator. Both of these can be circumvented with the use of surfactant hosts or polymer-based matrices.[8] Kim and coworkers have reported photochemical upconversion in nanocapsulated materials in water that was later used in photocatalysis.[17] These encapsulated materials contain a solution of sensitizer and acceptor pair in an organic solvent retaining the favorable photophysical properties but does not interact with the outside aqueous environment. Kimizuka and collaborators have demonstrated upconverted emission in aerated water by exploring triplet energy migration in an amphiphilic molecular self-assembled environment.[18] The chromophores self-assembled in the hydrophobic interior were developed using hydrogen bond networks of aqueous assembly systems that are less influenced by dissolved molecular oxygen.[19] Similar strategies such as encapsulation or adding oxygen scavengers were adopted by different groups to protect the triplet excited states against deactivation pathways by molecular oxygen.[20-23] More recently, Congreve and coworkers demonstrated that the addition of a high-boiling solvent as a swelling agent in the micelle interior could dramatically improve efficiency of a fully micelle-encapsulated TTA-UC system.[24] In 2017, the Castellano group reported on the first contribution of upconversion in neat water using combinations of water-soluble Ru(II) MLCT sensitizers in concert with 9-anthracenecarboxylate ($AnCO_2^-$) and 1-pyrenecarboxylate ($PyCO_2^-$).[25] Following this work, Kerzig et al. synthesized water-soluble Ru(II)[26] and Ir(III) photosensitizers, which could sensitize

commercially available anthracene and naphthalene annihilators, respectively.[15] These systems were used for aqueous TTA-UC in the UV as well as to drive thermodynamically challenging carbon–chlorine bond activation for purifying water from halogenated contaminants.

In the current report, we execute TTA-UC from a Cu(I) MLCT excited state in water for the first time. In this study, $[Cu(dsbtmp)_2]PF_6$ (Cu-PS) was used as the photosensitizer, and the water-soluble sodium 10-phenylanthracene-9-carboxylate (PAC) was used as the triplet acceptor/annihilator. To facilitate the incorporation of the water-insoluble Cu-PS, the commercially available surfactant cetyltrimethylammonium bromide (CTAB) was added to the aqueous solution as a host. The micellar design and the molecular structures of the different components are presented in **Figure 1**.

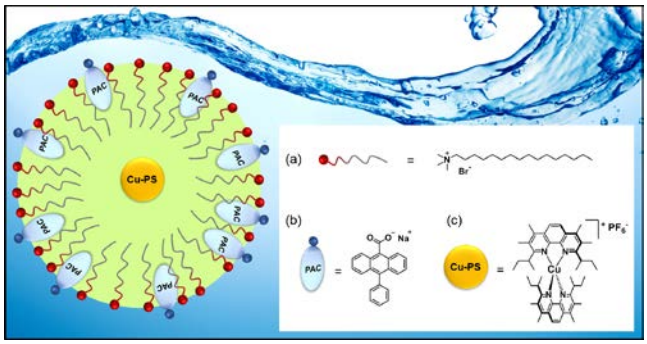

Figure 1. Proposed configuration of the assembly and chemical structures of CTAB (a), PAC (b) and Cu-PS (c).

Experimental

General. Spectrophotometric grade dichloromethane (DCM), and cetyltrimethylammonium bromide (CTAB) were purchased and used without further purification. $[Cu(dsbtmp)_2](PF_6)$ (Cu-PS) was available from previous studies.[27]

Synthesis of PAC Acceptor. The anthracene-based acceptor was prepared from the corresponding acid as follows. 10-phenyl-anthracene-9-carboxylic acid was prepared following a literature procedure.[28] The acid was then deprotonated by titrating with NaOH. In a round-bottom flask, 10-phenyl-anthracene-9-carboxylic acid (170 mg, 0.570 mmol, 1 eq) was first solubilized in ethanol (5 mL); 22.8 mg of NaOH (0.570 mmol, 1 eq) were dissolved in 5 mL of deionized water and added dropwise to the ethanol solution under stirring until the pH = 7. The resulting mixture was stirred for 30 min then evaporated under reduced pressure. The crude product was solubilized in water and filtered. After evaporation, the filtrate gave the desired compound as a crystalline light-yellow solid in 93% yield (170 mg, 0.530 mmol). ^{1}H NMR (400 MHz, D_2O) δ 8.12 (d, J = 8.7 Hz, 2H), 7.67 (d, J = 8.9 Hz, 2H), 7.64 – 7.55 (m, 5H), 7.45 – 7.36 (m, 4H). $^{13}C\{^1H\}$ NMR (100 MHz, D_2O) δ 178.8, 139.0, 137.4, 137.1, 131.8, 130.0, 129.2, 128.4, 127.2, 126.7, 126.4, 126.1.

Characterization of the Assembly. The viscosity of the samples was measured at 25°C by a DHR-2 rheometer (TA instruments), equipped with a Peltier Plate lower geometry and sand-blasted plate (50 mm) with cone (1 degree angle) for the upper geometry. ^{1}H DOSY NMR measurements were performed at 298 K on a Bruker Avance III NMR spectrometer operating at 700 MHz and equipped with a Bruker multinuclear z-gradient inverse probe head capable of producing gradients in the z direction with strength of 48 G cm^{-1}. The DOSY spectra were acquired with the ledbpgp2s pulse program available in the Bruker Topspin software. All spectra were recorded with 33 K time domain data points in the t_2 dimension and 20 t_1 increments. The gradient strength was square root incremented in 20 steps from 2% up to 98% of the maximum gradient strength. All measurements were performed with a compromise diffusion delay D of 60 ms in order to maintain the relaxation contribution to the signal attenuation constant for all samples. The gradient pulse length d was 3 ms in order to ensure full signal attenuation. The diffusion dimension of the 2D DOSY spectra was processed by means of MestReNova (version 10.0.2).

Static Absorption and Photoluminescence Spectroscopy. Spectroscopic measurements were performed in custom 1 cm^2 quartz optical cell with a side arm round-bottom flask and degassed by a freeze-pump-thaw technique for at least 3 cycles (See **Fig S13**). Static absorption spectra were measured with a Shimadzu UV-3600 spectrophotometer. Steady state photoluminescence emission spectra were obtained on a FLS920 fluorometer (Edinburgh Instruments). The concentration of sensitizer was chosen to give an absorbance of 0.1−0.2 at the excitation wavelength. The sample was excited with a 450 W Xe arc lamp, and the emission signal was detected with a Peltier cooled, red sensitive PMT (R2658P Hamamatsu).

Luminescence quantum yields Φ were measured in optically dilute water solution at absorbance values below 0.1 using $\Phi_S = \Phi_{ref} \times [(Grad_S/Grad_{ref}] \times [n_S^2/n_{ref}^2]$ where Grad is the gradient from the plot of integrated fluorescence intensity vs absorbance at excitation wavelength, and n the refractive index of the solvent. "ref" and "S" denote reference and sample respectively. Here, quantum yields were determined relative to quinine bisulfate in aerated 1 N aqueous sulfuric acid solution (Φ_{ref} = 0.546).

For power dependence studies, solutions were measured in custom-made air-free 1 cm^2 quartz optical cells. The concentration of acceptor was chosen to quench the sensitizer by at least 90%, according to the measured K_{SV}. Samples were excited with a 488 nm line of an Ar^+/ Kr^+ ion laser (Innova 70C Coherent), focused to a ~1.25 mm spot. The excitation power was measured using a Nova II/PD300-UV power meter/detector (Ophir). The excitation beam was filtered with a 488 nm notch filter. The upconverted emission intensity was recorded with the FLS920 fluorometer described above. The excitation power was varied with the use of neutral density filters which were placed after the excitation source. The average emission intensities were plotted versus the measured excitation power density.

Transient Absorption Spectroscopy. Transient absorption and time-resolved photoluminescence emission decays were collected with an LP920 laser flash photolysis system (Edinburgh Instruments). The excitation source was the Vibrant 355 LD-UVM Nd:YAG/OPO system (OPOTEK), and data acquisition was controlled by the L900 software program (Edinburgh Instruments). Kinetic traces were collected with a PMT (R928 Hamamatsu) and fitted using IGOR Pro and MATLAB, with the first 20 ns trimmed for the instrument response.

Samples were prepared by dissolving the Cu PS in 0.1 mL DCM which was subsequently added dropwise while stirring to a 5 mL aqueous CTAB solution (10 mM). The PAC annihilator was then added to the solution prior to performing all measurements.

Results and Discussion

Characterization of the Assembly. CTAB is a cationic surfactant and has a critical micellar concentration of 1 mM.[29] The radius of the micelles was calculated from the Stokes-Einstein relation (**Equation 1**), where r_h is the hydrodynamic radius, *k* is Boltzmann constant, T is the temperature, η is the viscosity and D_o is the diffusion coefficient which was determined by DOSY ^{1}H NMR. The hydrodynamic radius was found to be 7-8 nm and confirmed by DLS (**Figure S1**).

$$r_h = \frac{kT}{3\pi\eta D_o} \quad \textbf{(1)}$$

At a 10 mM concentration of CTAB, the aggregation number is known to be 75,[30] leading to a concentration of micelles of 120 μM (see SI). We note that the concentration employed is far below the limit of elongated[31] or elipsoidal[32] micelles and thus the micelles are assumed to be spherical in shape. The addition of the photosensitizer and annihilator to the CTAB solution did not alter the size of the micelles as apparent from the ^{1}H DOSY NMR spectra (**Figures S1** and **S2**) which appear at the same diffusion coefficient as the proton resonances in the aromatic region associated with Cu-PS and PAC. The resulting yellow solution also appeared transparent, indicating that the photosensitizer and annihilator are completely solvated. From the extracted diffusion coefficients of the different ^{1}H NMR signals, it can be inferred that both Cu-PS and PAC are associated with the CTAB assembly.

Static Spectroscopy. The steady-state absorption and photoluminescence (PL) spectra of Cu-PS and PAC in CTAB are presented in **Figure 2**. Cu-PS exhibits a broad and featureless MLCT absorption and red PL centered at 630 nm, consistent with what has been previously described.[27]

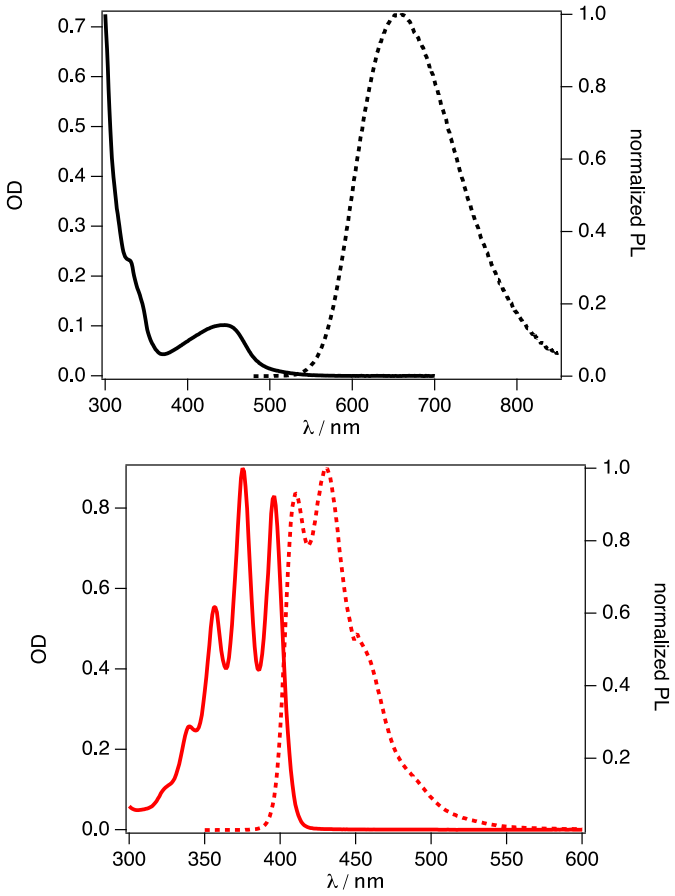

Figure 2. Steady-state absorption (solid line) and photoluminescence (dashed line) of 1.7 μM Cu-PS excited at 450 nm (top) and 0.1 mM PAC excited at 340 nm in 10 mM CTAB aqueous solution (buttom).

The finger-like vibronic bands shown in the absorption and PL are characteristic to the PAC annihilator with an intrinsically small Stokes shift. The additive nature of the absorption spectra when both Cu-PS and PAC are in solution indicates the absence of electronic coupling between the two independent chromophores (**Figure S3**).

Unlike previous reports,[33] which demonstrated that switching to D_2O increased the lifetimes resulting from the reduced vibrational coupling with the solvent, the Cu-PS lifetime did not change significantly when D_2O was substituted for H_2O suggesting that the Cu-PS is buried in the hydrophobic core of the assembly (**Figure S4)**. **Figure 3** presents the normalized single-wavelength kinetics of both the TA decay and the PL intensity decay monitored at 565 nm and 630 nm, respectively, for the Cu-PS in CTAB.

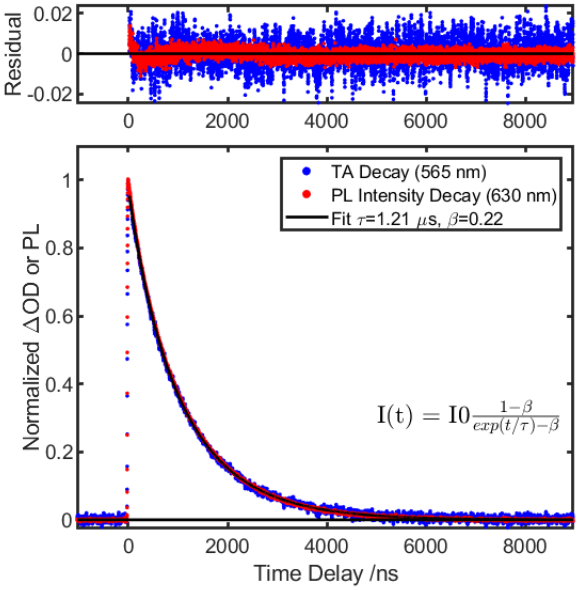

Figure 3. Normalized single-wavelength kinetics of Cu-PS, transient absorption decay detected at 565 nm (blue trace) and photoluminescence decay detected at 630 nm (red trace). Both traces fit to the model in Equation 2 with a 1.21 μs lifetime.

Owing to the inhomogeneity in the microenvironment of these self-assembled micellar assemblies in which the Cu-PS is localized, a simple single-exponential fit is not ideal for the excited state decays. At the concentrations used in **Figure 3**, and assuming a Poisson distribution of Cu-PS among the assemblies, 22% of the Cu-PS are in assemblies with at least two Cu-PS. In the close confines of a multiply occupied assembly, self-quenching is highly likely, leading to an apparent reduction in the luminescence. This self-quenching process will manifest as a second-order decay in addition to the first-order decay that occurs due to the inherent lifetime of the Cu-PS within the CTAB assembly. The functional form of dynamics that occur by parallel first- and second-order decays is known to be as follows:[34]

$$I(t) = I_0 \frac{(1-\beta)}{expexp\,(t/\tau) - \beta} \qquad \textbf{(2)}$$

Where $$\beta = \frac{k_{sec.\ order}[^3ES^*]_0}{k_{first\ order} + k_{sec.order}[^3ES^*]_0} \qquad \textbf{(3)}$$

In **Equation 2**, above, the luminescence intensity *I* is tracked relative to a time delay after the excitation pulse, *t*. I_0 is the initial emission intensity, τ is the lifetime of Cu-PS in the limit where all the Cu-PS is in singly occupied assemblies, and β is the fraction of decay that occurs via the second-order path. $[ES]_0$ represents the initial population of excited states generated by the excitation pulse. In this case, β is equivalent to the number of assemblies with more than one Cu-PS. Both decays are adequately fit to this model with a τ of 1.21 μs and a value of β of 0.22, exactly matching the fraction of multiply occupied assemblies predicted above from simple Poisson statistics.

Bimolecular Quenching Studies. Anthracene and its derivatives are frequently invoked as triplet annihilators, due to favorable energetics of their lowest energy triplet and singlet excited states and long triplet lifetimes, and have been successfully applied in

upconversion with various transition metal sensitizers including Ru(II), Pt(II), Pd(II) and Cu(I).[35] In this study, PAC was selected due to its solubility in water and relatively high fluorescence quantum yield, equal to 71% (**Figure S5**). In this system, standard Stern-Volmer modeling is not appropriate given that the PAC and Cu-PS are both associated with the assembly. An appropriate model is the one proposed by Turro and coworkers, which supposes that the distribution of quenchers among assemblies is governed by a Poisson distribution and that each quencher on an assembly has equal an independent likelihood of quenching the Cu-PS on the interior:[36]

$$\frac{I}{I_0} = e^{-<q>} * \sum_{q=0} \frac{<q>^q}{(1+q*K_{SV})*q!} \qquad \textbf{(4)}$$

where I and I_0 are the integrated sensitizer emission intensities in the presence and absence of annihilator, respectively, K_{SV} is the Stern-Volmer constant and is equal to $k_q*\tau_0$, and $<q>$, the average number of quenchers per assembly, is simply calculated in terms of the concentration of the quencher and the concentration of the assemblies (**Equation S3**). This model is appropriate for systems in which the quencher is fully micellized and luminescence decay in the presence of quencher is non-exponential. This is the case for the Cu-PS/CTAB/PAC system given the DOSY results above and luminescence decay kinetics (discussed below). Fitting of the data in **Figure S6** to this model yields a K_{SV} of 1.72, corresponding to a k_q of $1.42*10^6$ s^{-1}. It should be noted that this k_q, which reflects the frequency of collisions between Cu-PS and individual quencher species, has units of s^{-1} instead of $M^{-1}s^{-1}$ and is comparable to similar quenching rate constants found for quenching relative to other micelle encapsulated sensitizers and surface bound quenchers.[37-38] As an independent confirmation of the suitability of this model, a time resolved emission trace of the Cu-PS in the presence of CTAB and PAC was fit, again to a model developed by Turro and coworkers,[35] yielding a K_{SV} of 1.71, very close to value from the static emission experiments (**Figure S7**). To provide context for this K_{SV} for comparison to other upconversion systems, a value of 1.72 corresponds to a quenching efficiency of 44% with as few as one quencher per assembly up to nearly 94% with 10 quenchers per assembly, based on **Equation 3**.

Transient Absorption Studies. The transient absorption difference spectra of the photosensitizer alone and the Cu-PS/PAC assembly in water are presented in **Figure 4**. The prompt TA difference spectrum of the photosensitizer is identical to what is observed in pure DCM,[27] exhibiting a ground state bleach centered at 450 nm and a double top positive feature between 500 and 600 nm previously assigned to the phenanthroline radical anion.[39] The TA spectra collected upon the addition of the annihilator show spectral evolution with an isosbestic point at 492 nm (**Figure S8**). The new feature at 420 nm is attributed to the $T_1 \longrightarrow T_n$ absorption of PAC.[40] This growth of this signal was accompanied by fast decay of the Cu-PS signals, both with the same time-constant of ~80 ns, providing further evidence of triplet-triplet energy transfer from the Cu-PS to the annihilator.

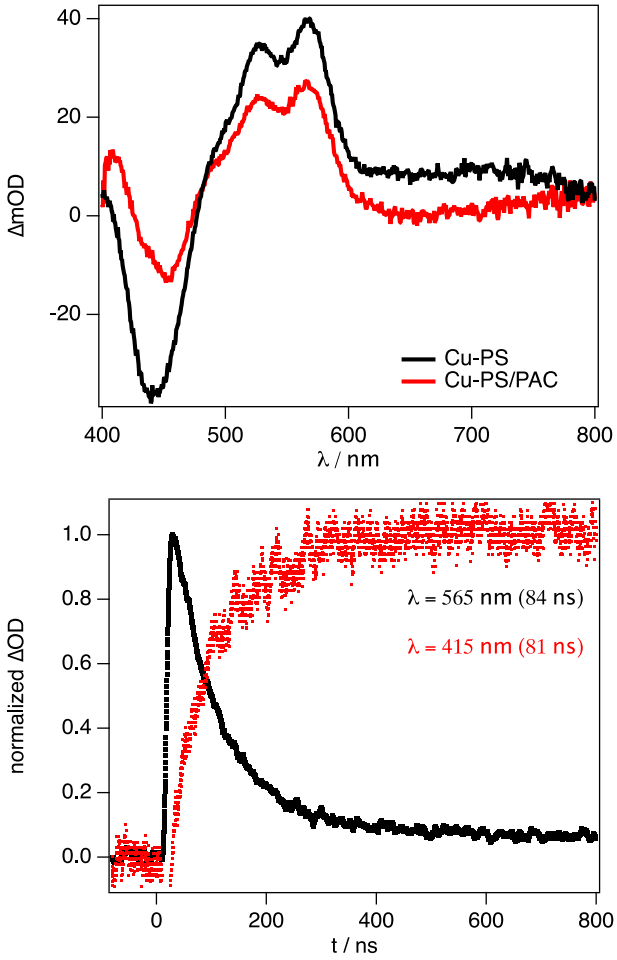

Figure 4. ns-TA of Cu-PS (black trace) and Cu-PS/PAC assembly (red trace) collected within 20 ns of the laser pulse (top). Cu-PS/PAC assembly transients collected at 565 nm (black trace) and 415 nm (red trace) showing the simultaneous decay of the PS triplet and the rise of the annihilator triplet (buttom). Samples were excited at 450 nm (2 mJ/pulse, O.D. = 0.43).

The kinetics of TTA were probed by measuring the decay of PAC $T_1 \longrightarrow T_n$ absorption signal (**Figure 5**). The transient decay was fit according to the model developed by Bachilo and Weisman.[34]

$$\left[{}^3PAC^*\right] = \left[{}^3PAC^*\right]_0 \frac{(1-\beta)}{exp\,(k_T t) - \beta} \qquad \textbf{(5)}$$

In **Equations 5** above, $[^3PAC^*]$ and $[^3PAC^*]_0$ represent the time-dependent and initial concentration of the annihilator triplet excited state, respectively. β was defined in **Equation 3** and in this case represents the fraction of initial decay that occurs through the TTA channel where $k_{first\ order}$ represents the first order triplet decay rate constant (k_T) and and $k_{sec.\ order}$ is the annihilation rate constant (k_{TTA}) and $[^3ES]_0$ is the concentration of PAC formed after the TTET event. The β value calculated here was 0.18 indicating that bimolecular triplet-triplet annihilation is 18% efficient with respect to all other triplet excited state decay processes.

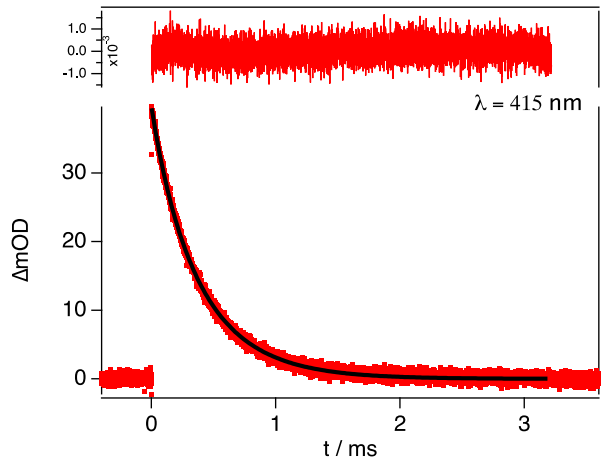

Figure 5. Single-wavelength kinetics collected at 415 nm for the Cu PS-PAC assembly showing the decay of the annihilator triplet. The decay was fitted according to model developed by Bachilo and Weisman.[40] Samples were excited at 450 nm (2 mJ/pulse, OD = 0.43).

This value is relatively low compared to other studies where typical values for efficient annihilation systems can be as high as 90% in organic solvents[35] and 75% in aqueous media.[26] The low β value might be partially attributable to the lack of mobility of the annihilators imposed by the latter's strong electrostatic attraction to the surfactant ultimately hindering the annihilation process. Furthermore, the quantum yield of the TTA process was found to be <1%. Substituting CTAB by Triton X-100, a neutral surfactant, resulted in β increasing by a factor of 1.7, supporting this hypothesis (**Figure S9**). The other factor that dictates β is $[^3PAC^*]_0$, which was calculated to be 210 μM based on the $\Delta A_0(^3PAC^*)$ and $\varepsilon(^3PAC^*)$ values (see SI). $[^3PAC^*]_0$ is smaller than in typical upconverting systems and is largely dictated by the ^3PS concentration. The extracted k_{TTA} rate constant from the fit of ΔOD was multiplied by $\varepsilon(^3PAC^*)$. The calculated value for k_{TTA}, 2.5×10^8 M^{-1} s^{-1}, is an order of magnitude below the diffusion limit in water, but is substantial considering it is expected to be limited by the diffusion of the assemblies and the affinity of the PAC for the positively charged CTAB headgroup. The combined results show that TTA in water is indeed achievable in the current aqueous assembly using a Cu(I) photosensitizer, but could be made more efficient by modifying the design to allow the annihilator to diffuse freely in the aqueous phase.

Incident Light Power Dependence The upconverted emission intensity is dependent on the population of the excited singlet state of the annihilator. The formation of the latter is dictated by two competing kinetic processes; the first order decay of the triplet (k_T) and the second order triplet-triplet annihilation reaction ($k_{TTA}[^3PAC^*]$). These two processes give rise to two kinetic regimes, which are expressed in their integrated forms in **Equations 6** and **7**. In the weak annihilation limit, where $k_T > k_{TTA}[^3PAC^*]$, the upconverted emission intensity exhibits a quadratic dependence on the excitation power density, **Equation 6**. However, at higher powers when $k_T < k_{TTA}[^3PAC^*]$, the triplet decay no longer limits annihilation and yield of upconversion becomes linear with excitation power density, **Equation 7**.

Weak annihilation regime $$N_F = \frac{\Phi_f k_{TTA}[^3PAC^*]_o^2}{2k_T} \quad \textbf{(6)}$$

Strong annihilation regime $$N_F = \Phi_f[^3PAC^*]_o \quad \textbf{(7)}$$

The double logarithmic plot of the upconverted intensity *vs* the power density is presented in **Figure 6**. The threshold power, which marks the transition between the weak and strong annihilation regimes, is the power at which the two fits intersect. Here, the threshold power is 7.73 W/cm^2.

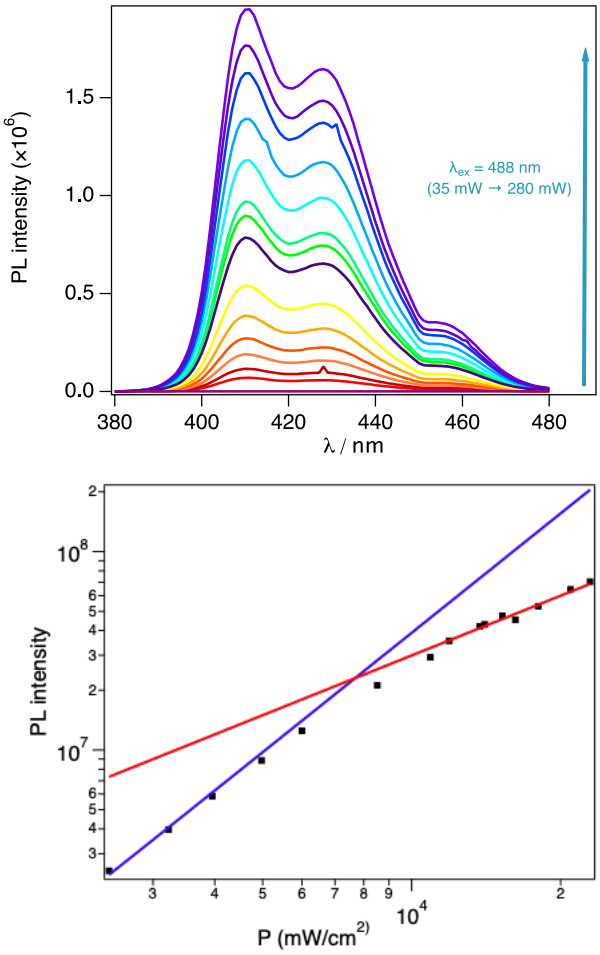

Figure 6. Power-dependence photoluminescence of Cu PS-PAC assembly excited with an Ar^+ laser at 488 nm (OD = 0.2) (top). Double logarithmic plot of PL vs power density, weak annihilation limit (blue fit) and strong annihilation limit (red fit) (buttom).

In addition to incident power, the concentration of the annihilator triplet excited state is also dictated by the concentration of the sensitizer at the excitation wavelength, assuming unity intersystem crossing and quantitative triplet-triplet energy transfer. A few reports have demonstrated that increasing the concentration of the sensitizer increases the annihilation events and hence the upconversion quantum yield.[41-42] Attempting to assess if this was operative in the Cu-PS/CTAB/PAC system, we studied the effect of sensitizer concentration on the threshold power. The sensitizer concentration was increased from 57 μM to 214 μM and surprisingly the threshold power density increased with increasing power density which implies a decrease in annihilation events, an increase in the first order triplet decay[43] or both. This likely stems from the fact that increasing the concentration of Cu-PS at a fixed concentration of CTAB increases the number of Cu-PS per assembly, increasing the extent of self-quenching, and reducing the yield of ^3PAC. Nonetheless, assuming that the threshold power scales up linearly with the sensitizer concentration, and comparing our assembly to that in pure DCM reported by McCusker et al. for the same copper complex with 1 W/cm^2 for 760 μM sensitizer (2,9-diphenylanthracene was used as the annihilator which has 1.33 times higher fluorescence quantum yield), one finds that the system nominally behaves equally or even slightly better to the one established in pure organic solvent.[14] Unfortunately, raising the sensitizer concentration above 214 μM renders the solution turbid and thus jeopardized our efforts

to study a micellar system with the same sensitizer concentration as the one previously reported.

Electron Transfer Studies Upconversion by TTA is not only useful for energy conversion applications but also valuable for driving energetically demanding (uphill) reactions that typically require UV light excitation. To test our Cu-PS/PAC assembly towards delivering this energy to the aqueous phase, methyl viologen (MV^{2+}) was added into the solution. MV^{2+} is a widely used electron acceptor having a relatively low LUMO energy with a reduction potential of -0.45 vs NHE.[44] In its reduced form, $MV^{+\cdot}$ has 2 characteristic absorption bands centered at 396 nm and 606 nm in water.[45] **Figure 7** presents the ns-TA difference spectrum of the Cu PS-PAC assembly in the presence of 10 mM MV^{2+} at different time delays. The prompt signal consists of the pure Cu(I) MLCT excited state, after which the long-lived triplet-to-triplet PAC absorption signal initially grows, centered at 420 nm. Although $MV^{+\cdot}$ has a strong absorption feature at 396 nm, it is somewhat masked by the overlapping PAC signal. However, on the 100 microsecond and longer timescale, the ^{3}PAC has decayed but the characteristic $MV^{+\cdot}$ visible bands can be observed. Reproducing the same experiment in the absence of the PAC, quenching of the Cu(I) MLCT excited state no longer occurs and no $MV^{+\cdot}$ transients are detected (**Figure S10**). This suggests that the Cu-PS is well shielded from the aqueous environment and not accessible to the MV^{2+}. Moreover, it shows that the PAC is necessary to gain access to the aqueous environment to enable chemistry at the CTAB/water interface. To gain insight into whether electrostatics play a role in the electron transfer, PAC was replaced by benzoate ($PhCOO^-$) (**Figure S10**). The $PhCOO^-$ triplet state is substantially higher in energy than the triplet of Cu-PS which renders TTET from Cu-PS thermodynamically unfavorable. The absence of quenching in this assembly by MV^{2+} further supports our finding that the PAC plays a key role in extracting and relaying the energy from within the assembly to the exterior aqueous environment, in which the electron transfer to MV^{2+} likely happens from the long-lived triplet excited state of PAC (**Figure S11**). Most importantly, the combined results from this experiment and DOSY NMR gives insight about the architecture of this assembly and suggests that Cu-PS is buried in the hydrophobic core of the assembly, while the PAC annihilator is likely decorating the surface of the assembly at the CTAB/water interface. This result may prove useful for photocatalytic applications, as it provides a scheme for protecting a sensitive photocatalyst in a surfactant assembly while efficiently shuttling the excitation energy into the aqueous medium outside of the assembly.

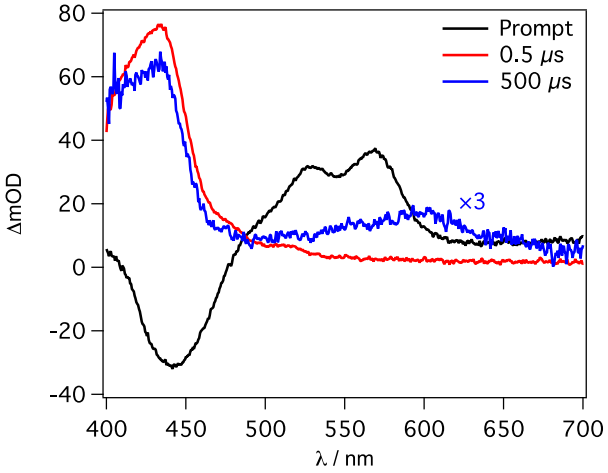

Figure 7. ns-TA spectra of Cu-PS/PAC assembly in the presence of MV^{2+} at different time delays, prompt (black trace) showing the Cu-PS transient, 0.5 μs (red trace) showing the PAC signal, 500 μs (blue trace) showing the $MV^{+\cdot}$ transient centered at 600 nm.

Conclusions

This study served as a proof-of-principle towards integrating earth-abundant molecules in non-toxic environments to generate high energy photons from visible light. The proposed design achieved efficient TTET rates, however the lack of PAC mobility and the requirement for low sensitizer concentrations adversely affected the annihilation process resulting in a relatively modest TTA yield. The combined experimental data illustrated that the surface bound annihilators were able to extract excited triplet energy from the Cu(I) photosensitizers contained within the surfactant assemblies, ultimately shuttling the excitation into the bulk aqueous solution through electron transfer. This is particularly important for remotely operating photoredox reactions in water while rendering the Cu(I) photosensitizer spatially confined in the hydrophobic core of the assemblies.

ASSOCIATED CONTENT

Supporting Information

The following files are available free of charge. DOSY NMR, micelle characterization and modeling, additional ns-TA data, PAC quantum yield and triplet epsilon calculation and NMR.

AUTHOR INFORMATION

Corresponding Author

Felix N. Castellano - Department of Chemistry, North Carolina State University, Raleigh, North Carolina 27695-8204, United States; Email: fncastel@ncsu.edu

Authors

Remi Fayad - Department of Chemistry, North Carolina State University, Raleigh, North Carolina 27695-8204, United States

Anh Thy Bui – Institut des Sciences Chimiques, Université de Rennes 1, Rennes, France

Samuel Shepard - Department of Chemistry, North Carolina State University, Raleigh, North Carolina 27695-8204, United States

ACKNOWLEDGMENT

We thank Dr. Peter Thompson for his help with the DOSY ^{1}H NMR experiment. The structural characterization aspects of the work were performed in part by the Molecular Education, Technology and Research Innovation Center (METRIC) at NC State University, which is supported by the State of North Carolina. We acknowledge support for this contribution from BioLEC, an Energy Frontier Research Center funded by the U.S. Department of Energy, Office of Science, Office of Basic Energy Sciences under Award no. DE-SC0019370. The synthesis of the water-soluble acceptor was funded by the U.S. Department of Energy, Office of Science, Office of Basic Energy Sciences, under Award Number DE-SC0011979.

REFERENCES

1. Pedrini, J.; Monguzzi, A., Recent advances in the application triplet-triplet annihilation-based photon upconversion systems to solar technologies. *Journal of Photonics for Energy* **2018,** *8* (2), 022005.
2. Dilbeck, T.; Hanson, K., Molecular Photon Upconversion Solar Cells Using Multilayer Assemblies: Progress and Prospects. *Journal of Physical Chemistry Letters* **2018,** *9* (19), 5810-5821.
3. Gholizadeh, E. M.; Prasad, S. K. K.; Teh, Z. L.; Ishwara, T.; Norman, S.; Petty, A. J.; Cole, J. H.; Cheong, S.; Tilley, R. D.; Anthony, J.

E.; Huang, S. J.; Schmidt, T. W., Photochemical upconversion of near-infrared light from below the silicon bandgap. *Nature Photonics* **2020,** *14* (9), 585-590.
4. Schulze, T. F.; Schmidt, T. W., Photochemical upconversion: present status and prospects for its application to solar energy conversion. *Energy & Environmental Science* **2015,** *8* (1), 103-125.
5. Liu, Q.; Yin, B.; Yang, T.; Yang, Y.; Shen, Z.; Yao, P.; Li, F., A General Strategy for Biocompatible, High-Effective Upconversion Nanocapsules Based on Triplet–Triplet Annihilation. *Journal of the American Chemical Society* **2013,** *135* (13), 5029-5037.
6. Wohnhaas, C.; Mailänder, V.; Dröge, M.; Filatov, M. A.; Busko, D.; Avlasevich, Y.; Baluschev, S.; Miteva, T.; Landfester, K.; Turshatov, A., Triplet–Triplet Annihilation Upconversion Based Nanocapsules for Bioimaging Under Excitation by Red and Deep-Red Light. *Macromolecular Bioscience* **2013,** *13* (10), 1422-1430.
7. Askes, S. H. C.; Bahreman, A.; Bonnet, S., Activation of a Photodissociative Ruthenium Complex by Triplet–Triplet Annihilation Upconversion in Liposomes. *Angewandte Chemie International Edition* **2014,** *53* (4), 1029-1033.
8. Askes, S. H. C.; Bonnet, S., Solving the oxygen sensitivity of sensitized photon upconversion in life science applications. *Nature Reviews Chemistry* **2018,** *2* (12), 437-452.
9. Huang, L.; Kakadiaris, E.; Vaneckova, T.; Huang, K.; Vaculovicova, M.; Han, G., Designing next generation of photon upconversion: Recent advances in organic triplet-triplet annihilation upconversion nanoparticles. *Biomaterials* **2019,** *201*, 77-86.
10. Parker, C. A.; Hatchard, C. G.; Joyce, T. A., Selective and Mutual Sensitization of Delayed Fluorescence. *Nature* **1965,** *205* (4978), 1282-1284.
11. Singh-Rachford, T. N.; Castellano, F. N., Photon upconversion based on sensitized triplet–triplet annihilation. *Coordination Chemistry Reviews* **2010,** *254* (21), 2560-2573.
12. Gray, V.; Moth-Poulsen, K.; Albinsson, B.; Abrahamsson, M., Towards efficient solid-state triplet–triplet annihilation based photon upconversion: Supramolecular, macromolecular and self-assembled systems. *Coordination Chemistry Reviews* **2018,** *362*, 54-71.
13. McCusker, C. E.; Castellano, F. N., Orange-to-blue and red-to-green photon upconversion with a broadband absorbing copper (I) MLCT sensitizer. *Chemical Communications* **2013,** *49* (34), 3537-3539.
14. McCusker, C. E.; Castellano, F. N., Efficient Visible to Near-UV Photochemical Upconversion Sensitized by a Long Lifetime Cu(I) MLCT Complex. *Inorganic Chemistry* **2015,** *54* (12), 6035-6042.
15. Pfund, B.; Steffen, D. M.; Schreier, M. R.; Bertrams, M.-S.; Ye, C.; Börjesson, K.; Wenger, O. S.; Kerzig, C., UV Light Generation and Challenging Photoreactions Enabled by Upconversion in Water. *Journal of the American Chemical Society* **2020,** *142* (23), 10468-10476.
16. Ravetz, B. D.; Pun, A. B.; Churchill, E. M.; Congreve, D. N.; Rovis, T.; Campos, L. M., Photoredox catalysis using infrared light via triplet fusion upconversion. *Nature* **2019,** *565* (7739), 343-346.
17. Kim, J.-H.; Deng, F.; Castellano, F. N.; Kim, J.-H., Red-to-Blue/Cyan/Green Upconverting Microcapsules for Aqueous- and Dry-Phase Color Tuning and Magnetic Sorting. *ACS Photonics* **2014,** *1* (4), 382-388.
18. Kimizuka, N.; Yanai, N.; Morikawa, M.-a., Photon Upconversion and Molecular Solar Energy Storage by Maximizing the Potential of Molecular Self-Assembly. *Langmuir* **2016,** *32* (47), 12304-12322.
19. Kouno, H.; Ogawa, T.; Amemori, S.; Mahato, P.; Yanai, N.; Kimizuka, N., Triplet energy migration-based photon upconversion by amphiphilic molecular assemblies in aerated water. *Chemical Science* **2016,** *7* (8), 5224-5229.
20. Mongin, C.; Golden, J. H.; Castellano, F. N., Liquid PEG Polymers Containing Antioxidants: A Versatile Platform for Studying Oxygen-Sensitive Photochemical Processes. *ACS Applied Materials & Interfaces* **2016,** *8* (36), 24038-24048.
21. Duan, P.; Yanai, N.; Kimizuka, N., Photon Upconverting Liquids: Matrix-Free Molecular Upconversion Systems Functioning in Air. *Journal of the American Chemical Society* **2013,** *135* (51), 19056-19059.
22. Kim, J.-H.; Kim, J.-H., Encapsulated Triplet–Triplet Annihilation-Based Upconversion in the Aqueous Phase for Sub-Band-Gap Semiconductor Photocatalysis. *Journal of the American Chemical Society* **2012,** *134* (42), 17478-17481.
23. Filatov, M. A.; Baluschev, S.; Landfester, K., Protection of densely populated excited triplet state ensembles against deactivation by molecular oxygen. *Chemical Society Reviews* **2016,** *45* (17), 4668-4689.
24. Sanders, S. N.; Gangishetty, M. K.; Sfeir, M. Y.; Congreve, D. N., Photon Upconversion in Aqueous Nanodroplets. *Journal of the American Chemical Society* **2019,** *141* (23), 9180-9184.
25. El Roz, K. A.; Castellano, F. N., Photochemical upconversion in water. *Chemical Communications* **2017,** *53* (85), 11705-11708.
26. Kerzig, C.; Wenger, O. S., Sensitized triplet–triplet annihilation upconversion in water and its application to photochemical transformations. *Chemical Science* **2018,** *9* (32), 6670-6678.
27. McCusker, C. E.; Castellano, F. N., Design of a Long-Lifetime, Earth-Abundant, Aqueous Compatible Cu(I) Photosensitizer Using Cooperative Steric Effects. *Inorganic Chemistry* **2013,** *52* (14), 8114-8120.
28. Zhu, L.; Al-Kaysi, R. O.; Dillon, R. J.; Tham, F. S.; Bardeen, C. J., Crystal Structures and Photophysical Properties of 9-Anthracene Carboxylic Acid Derivatives for Photomechanical Applications. *Crystal Growth & Design* **2011,** *11* (11), 4975-4983.
29. Li, W.; Zhang, M.; Zhang, J.; Han, Y., Self-assembly of cetyl trimethylammonium bromide in ethanol-water mixtures. *Frontiers of Chemistry in China* **2006,** *1* (4), 438-442.
30. Pisárčik, M.; Devínsky, F.; Pupák, M., Determination of micelle aggregation numbers of alkyltrimethylammonium bromide and sodium dodecyl sulfate surfactants using time-resolved fluorescence quenching. *Open Chemistry* **2015,** (1).
31. Reiss-Husson, F.; Luzzati, V., The Structure of the Micellar Solutions of Some Amphiphilic Compounds in Pure Water as Determined by Absolute Small-Angle X-Ray Scattering Techniques. *The Journal of Physical Chemistry* **1964,** *68* (12), 3504-3511.
32. Berr, S.; Jones, R. R. M.; Johnson, J. S., Effect of counterion on the size and charge of alkyltrimethylammonium halide micelles as a function of chain length and concentration as determined by small-angle neutron scattering. *The Journal of Physical Chemistry* **1992,** *96* (13), 5611-5614.
33. Sriram, R.; Hoffman, M. Z., Solvent isotope effect on the photophysics of $Ru(bpy)_3^{2+}$ and $Ru(phen)_3^{2+}$ in aqueous solution at room temperature. *Chemical Physics Letters* **1982,** *85*, 572-575.
34. Bachilo, S. M.; Weisman, R. B., Determination of Triplet Quantum Yields from Triplet−Triplet Annihilation Fluorescence. *The Journal of Physical Chemistry A* **2000,** *104* (33), 7711-7714.
35. Castellano, F. N.; McCusker, C. E., MLCT sensitizers in photochemical upconversion: past, present, and potential future directions. *Dalton Transactions* **2015,** *44* (41), 17906-17910.
36. Yekta, A.; Aikawa, M.; Turro, N. J., Photoluminescence methods for evaluation of solubilization parameters and dynamics or micellar aggregates. Limiting cases which allow estimation of partition coefficients, aggregation numbers, entrance and exit rates. *Chemical Physics Letters* **1979,** *63* (3), 543-548.
37. Atik, S. S.; Singer, L. A., A comparison of approximate and exact statistical models for intramicellar fluorescence quenching. *Chemical Physics Letters* **1979,** *66* (2), 234-237.
38. Dederen, J.; Van der Auweraer, M.; De Schryver, F., Fluorescence quenching of solubilized pyrene and pyrene derivatives by metal ions in SDS micelles. *The Journal of Physical Chemistry* **1981,** *85* (9), 1198-1202.
39. Palmer, C. E. A.; McMillin, D. R.; Kirmaier, C.; Holten, D., Flash photolysis and quenching studies of copper(I) systems in the presence of Lewis bases: inorganic exciplexes? *Inorganic Chemistry* **1987,** *26* (19), 3167-3170.
40. Porter, G.; Wilkinson, F., Energy transfer from the triplet state. *Proceedings of the Royal Society of London. Series A. Mathematical and Physical Sciences* **1961,** *264* (1316), 1-18.
41. Tayebjee, M. J. Y.; McCamey, D. R.; Schmidt, T. W., Beyond Shockley–Queisser: Molecular Approaches to High-Efficiency Photovoltaics. *The Journal of Physical Chemistry Letters* **2015,** *6* (12), 2367-2378.
42. Frazer, L.; Gallaher, J. K.; Schmidt, T. W., Optimizing the Efficiency of Solar Photon Upconversion. *ACS Energy Letters* **2017,** *2* (6), 1346-1354.
43. Gholizadeh, E. M.; Frazer, L.; MacQueen, R. W.; Gallaher, J. K.; Schmidt, T. W., Photochemical upconversion is suppressed by high concentrations of molecular sensitizers. *Physical Chemistry Chemical Physics* **2018,** *20* (29), 19500-19506.
44. Kavarnos, G. J.; Turro, N. J., Photosensitization by reversible electron transfer: theories, experimental evidence, and examples. *Chemical Reviews* **1986,** *86* (2), 401-449.
45. Watanabe, T.; Honda, K., Measurement of the extinction coefficient of the methyl viologen cation radical and the efficiency of its

formation by semiconductor photocatalysis. *The Journal of Physical Chemistry* **1982,** *86* (14), 2617-2619.